Journal of Sound and Vibration (2001) **239**(2), 217–231
doi:10.1006/jsvi.2000.3170, available online at http://www.idealibrary.com on IDEAL®

RESPONSE ANALYSIS OF TUNED MASS DAMPERS TO STRUCTURES EXPOSED TO VORTEX LOADING OF SIMIU–SCANLAN TYPE

L. Andersen, N. W. Birch, A. H. Hansen and J.-O. Skibelund

Department of Building Technology and Structural Engineering, Aalborg University, Sohngaardsholmsvej 57, *DK*-9000 *Aalborg, Denmark. E-mail: la@civil.auc.dk*

(*Received* 9 *April* 1999, *and in final form* 28 *April* 2000)

Vortex-induced loads on slender one-dimensional structures vibrating at lock-in conditions consist of a self-induced part in phase with the velocity of the structure in addition to an additive, almost harmonially varying component representing the same type of load as the vortex-induced force on a fixed cylinder. Simiu and Scanlan (1996 *Wind Effects on Structures*. New York: John Wiley & Sons Inc.) have proposed a widely used model for the self-induced part of the load based on a van der Pol oscillator. The aim of this paper is to investigate the optimal design of tuned mass dampers for such a load model. The method of analysis is based on the averaging method (Krylov–Bogoliubov–Mitropolsky first order perturbation analysis) for weakly non-linear systems. Several interesting findings have come out of the analysis. First, it is shown that, if the additive loading is omitted, the vibrations will be completely removed in an interval of the frequency tuning in contrast to the case of harmonic loading, where total damping of the primary system at optimal tuning is only possible when no structural damping is present. The stability of the theoretically possible motions is checked at different levels of viscous damping in the tuned mass damper. From this analysis it is concluded that introducing less damping than used for harmonic load, in order to achieve optimal results, may prove more efficient as far as van der Pol oscillator load model is concerned. The theory has been applied to passive damping control of the Rio–Niterói steel girder bridge, Rio de Janeiro, which is occasionally severely exposed to vortex-induced vibrations.

1. INTRODUCTION

Vortex-induced loads may influence the response of slender one-dimensional structures with low structural damping such as steel bridge decks and steel chimneys under certain conditions. When the Strouhal vortex-shedding frequency is close to one of the natural frequencies of the structure, the vortex shedding may be controlled by the structure at the natural frequency leading to large resonant vibrations. This synchronization of the vortex-shedding frequency and one of the natural frequencies is known as frequency lock-in.

At lock-in, a self-induced load component in phase with the structural velocity is built up in addition to the vortex-induced, almost harmonially varying load. The self-induced load acts as an equivalent negative viscous damping at small vibration levels which will further enhance the response level of the structure, especially if the structural damping is relatively small. The self-induced load is known to diminish as the vibration load increases. Physically, this self-limitation has been explained as the shedding of more than two vortices per vibration period at sufficiently large vibration levels, resulting in a non-resonant excitation [2]. A thorough analysis of this fluid–structure interaction problem requires the

0022-460X/01/020217 + 15 $35.00/0

integration of the Navier–Stokes equations. Although this has become possible, at least for two dimensional (2D) flow conditions, it is still a large computational task. For this reason a number of simplified models have been suggested in the literature. Starting with Hartlen and Currie [3], the so-called wake oscillator models were formulated, where a linear single-degree-of-freedom (SDOF) oscillator representing the structure interacts with a non-linear oscillator representing the oscillations of the surrounding fluid. Later modifications to this concept were due to Skop and Griffin [4], who tried to improve the predictions of the model by introducing a non-linear spring stiffness, and by Iwan and Blevins [5], who attempted to derive the wake oscillator equations from momentum balancing equations for the near-flow field. An extensive review of these efforts as well as their shortcomings was given by Sarpkaya [6]. Recently, Krenk and Nielsen [7] have suggested a simple modification of the wake oscillation equations, where the idea is that the coupling terms between the two oscillators should represent the balance of energy flowing between the two systems. With this modification, they were able to show that many of the shortcomings of earlier formulations of wake oscillator models in predicting the length of the lock-in interval the amplitude hysteresis at change of the wind velocity, etc., could be overcome.

Alternatively, a simple model has been suggested by Simiu and Scanlan [1] where the self-induced and self-limiting load component is modelled by a van der Pol oscillator. With suitable calibration, amplitude data can be represented quite accurately by this model. The odel has been further elaborated and verified by Goswami *et al.* [8, 9] and Larsen [10]. Due to its simplicity and accuracy this model has been adopted for the vortex-induced load in this study.

The vibration problem due to lock-in has been solved for steel chimneys by implementation of different damping devices and helical strakes; see, for example, Dyrbye and Hansen [11]. A number of modern high-rise buildings such as the John Hancock Tower in Boston and the Crystal Tower in Kobe, have also been equipped with control systems to prevent vibrations (see, for example, Connor and Klink [12]). Furthermore, great interest has recently been given to damping of vortex-induced vibrations on bridge decks. An example is the East Bridge approach spans of the Great Belt Bridge, Denmark (see, for example, Livesey and Larose [13]).

Given the quasi-harmonic nature of the vibrations that occur at lock-in, an obvious choice of vibration control is the use of tuned mass dampers (see, for example, Korenev and Reznikov [14]). This relatively simple form of passive dynamic control is obtained by attaching a control mass to the main structure using a spring and damping device and assuming viscous damping. The three parameters, mass, spring stiffness and damping coefficient, must be tuned for optimal performance of the control system.

Alternatively, an active or semi-active control system can be used although it should be kept in mind that active control is dependent on external energy supply. Batista and Pfeil [15] have shown that further reduction of the vortex-induced vibrations on a bridge deck can be achieved in this way. In this paper, however, passive, dynamic control with tuned mass dampers will be considered, where a novel approach to the optimization problem is carried out. The Simiu–Scanlan load model is used. Here no extra degree of freedom is associated with the vortices: thus the mechanical system of the structure and fluid flow reduces to a SDOF system. This simplifies the optimization process with respect to damping of the motion.

2. DETERMINISTIC MODEL OF VORTEX-INDUCED WIND LOAD ON BRIDGE DECK

The response of a structure subjected to aerodynamic load depends on the aerodynamic interaction between the flow and the structure itself. When the structure is at rest the

circular frequency of vortex-induced excitation, Ω_s, is governed by the Strouhal relation

$$\Omega_s = 2\pi SU/D. \tag{1}$$

Here S is the Strouhal number which depends on the Reynolds number and the shape of the cross-section; i.e., the frequency of the vortex separation is proportional to the wind velocity. U is the velocity of the flow and D is the across-stream dimension of the structure. However, when the Strouhal frequency, Ω_s, approaches one of the circular eigenfrequencies, ω, of the structure the vortex-shedding frequency will no longer depend on the wind velocity, but is controlled by the structure at the eigenfrequency (see Figure 1). In general, the tendency to enter a state of the lock-in interval depends on the Scruton number, i.e., a non-dimensional expression of the structure damping (see, for example, Dyrbye and Hansen [11]).

Assuming constant wind velocity, the resulting vibrations at lock-in with time approach a stationary motion with a dominant harmonic composant. In the following, it is assumed that the structural damping is low which is generally the case for steel and pre-stressed steelwire concrete structures.

A slender one-dimensional structure such as a chimney or bridge deck is considered. Since lock-in is a resonance phenomenon the motion is dominated by a single mode, i.e., the motion of the deck in the direction of the vortex-induced load may be written as

$$z(x, t) \simeq \phi(x)\, q(t), \tag{2}$$

where $z(x, t)$ is the displacement, x is the along-span co-ordinate, $\phi(x)$ is the mode shape related to the dominant eigenmode with circular eigenfrequency and $q(t)$ is the corresponding modal co-ordinate.

Introducing a control system (a tuned mass damper) at the location $x = x_c$ and taking into account the effect of vortex-induced load on the structure, the equation of motion for the primary system (bridge) takes the form

$$\ddot{q} + 2\zeta\omega\dot{q} + \omega^2 q = \frac{1}{M}(F_c + F_a), \tag{3}$$

where $\ddot{q}$ and $\dot{q}$ denote the modal acceleration and velocity of the deck, respectively, ζ is the modal damping ratio corresponding to the dominant eigenmode, ω is the corresponding

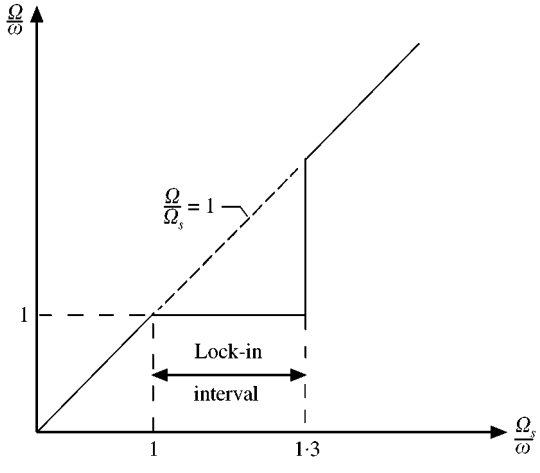

Figure 1. Lock-in. The circular vortex-shedding frequency, Ω, and Strouhal frequency, Ω_s, are standardized with respect to the circular eigenfrequency, ω. The length of the lock-in interval depends on the Scruton number.

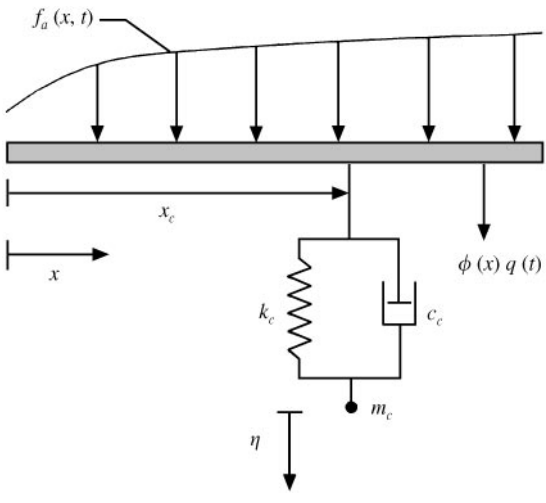

Figure 2. Mechanical system with definition of loading, displacements and dynamic properties.

circular eigenfrequency and M represents the modal mass when no control system is attached, F_c is the modal control force originating from the tuned mass damper (Figure 2), and

$$F_c = m_c[2\zeta_c\omega_c(\dot{\eta} - \phi(x_c)\dot{q}) + \omega_c^2(\eta - \phi(x_c)q)]\phi(x_c). \tag{4}$$

Here $\zeta_c = c_c/2m_c\omega_c$ and ω_c signify the damping ratio and circular eigenfrequency of the control system, respectively, when the primary system is fixed. η and $\dot{\eta}$ are the displacement and the velocity of the control mass, m_c (secondary system).

F_a is the modal aerodynamic load on the deck. Simiu and Scanlan [1] have suggested the following van der Pol model for the vortex-induced load per unit length of a structure at lock-in,

$$f_a(x, t) = \tfrac{1}{2}\rho U^2 D\left(Y_1(K)\left(1 - \varepsilon\frac{z^2}{D^2}\right)\frac{\dot{z}}{U} - Y_2(K)\frac{\ddot{z}}{\Omega^2 D} + C_L(K)\cos(\Omega t + \theta)\right), \tag{5}$$

where ρ is the air density, U is the mean wind-flow velocity, D is the across-flow dimension of the structure, Y_1, Y_2 and ε are positive, non-dimensional fitting parameters, C_L is the lift coefficient, and Ω is the circular shedding frequency. $K = \omega/\Omega_s$ is the reduced frequency, $\dot{z}$ is the vertical velocity of the structure, and θ is a phase shift to be specified below.

The first term of equation (5) is a measure of the negative aerodynamic damping which is subtracted from the structural damping thus bringing the system into the form of a van der Pol oscillator. The last term of equation (5) is the additive (external) load similar to the load that acts on a fixed structure. The middle term of equation (5) is supposed to describe the force of inertia from the added mass.

Assuming full spanwise correlation of the aerodynamic force and ignoring the contribution from aerodynamic inertia which is insignificant in proportion to aerodynamic damping, the modal load becomes

$$F_a = \tfrac{1}{2}\rho U^2 D\left(Y_1\left(\alpha_2 - \alpha_4\varepsilon\frac{q^2}{D^2}\right)\frac{\dot{q}}{U} + \alpha_1 C_L\sin(\Omega_s t + \theta)\right), \tag{6}$$

where

$$\alpha_n = \int_0^l \phi^n(x)\,\mathrm{d}x$$

with l being the length of the structure. In practice, however, full spanwise correlation is not possible. At lock-in the motion of the bridge deck controls the vortex shedding. This means that approximately full correlation will occur where the amplitudes are at their maximum, while the vortex shedding at the supports will be more chaotic. Thus, it seems reasonable to assume full spanwise correlation.

Simiu and Scanlan [1] have suggested that the additive lift coefficient term may be omitted in the case of lock-in. This omission leads to reasonable results when no control system is present since the negative aerodynamic damping term of equation (6) is dominant [1]. Nevertheless, an optimized passive control system may be able to dissipate more energy than induced by the motion of the structure due to the negative aerodynamic damping. Hence, it will be shown below that omission of the lift coefficient term under these conditions results in complete extinction of vibrations in both the primary and secondary systems. Consequently, the additive load term should be included in the optimal design procedure.

Inserting equations (4) and (6) into equation (3) gives

$$\ddot{q} + 2\omega\left(\zeta - \frac{\rho U D Y_1}{4\omega M}\left(\alpha_2 - \alpha_4 \varepsilon \frac{q^2}{D^2}\right)\right)\dot{q} + \omega^2 q$$

$$= \frac{m_c}{M}[2\zeta_c\omega_c(\dot{\eta} - \phi(x_c)\dot{q}) + \omega_c^2(\eta - \phi(x_c)q)]\phi(x_c) + \frac{1}{2M}\alpha_1 \rho U^2 D C_L \cos(\Omega t + \theta). \tag{7}$$

For the secondary system (i.e., the control system) the equation of motion takes the form

$$m_c(\ddot{\eta} + 2\zeta_c\omega_c(\dot{\eta} - \phi(x_c)\dot{q}) + \omega_c^2(\eta - \phi(x_c)q)) = 0. \tag{8}$$

The equations of motion are reformulated as

$$\ddot{\chi} + 2\omega_0\left(\zeta_0 - \zeta_1\left(1 - \varepsilon_D \frac{\chi^2}{D^2}\right)\right)\dot{\chi} + \omega_0^2\chi = v(\omega_c^2\eta + 2\zeta_c\omega_c\dot{\eta}) + F_0\cos(\Omega t + \theta),$$
$$\ddot{\eta} + 2\zeta_c\omega_c\dot{\eta} + \omega_c^2\eta = \omega_c^2\phi\chi + 2\zeta_c\omega_c\phi\dot{\chi}, \tag{9}$$

where

$$\chi = \phi(x_c)q, \quad \omega_0^2 = \omega^2\left(1 + \frac{\omega_c^2}{\omega^2}v\right), \quad v = \frac{\phi^2 m_c}{M}, \quad 2\zeta_0\omega_0 = 2\zeta\omega + 2\zeta_c\omega_c v,$$
$$2\zeta_1\omega_0 = \frac{\alpha_2\rho U D Y_1}{2M}, \quad \varepsilon_D = \frac{\alpha_4}{\alpha_2}\phi^2(x_c)\varepsilon, \quad F_0 = \frac{1}{2M}\phi(x_c)\alpha_1\rho U^2 D C_L. \tag{10}$$

3. TRANSFORMATION TO VAN DER POL CO-ORDINATES

After some time the motion of the system becomes periodic with period T and with a dominant harmonic composant with the circular frequency Ω. Notice that the circular frequency of the motion is identical to the excitation frequency of the additive load.

In order to analyse this harmonic component it is useful to perform a transformation from physical-state variables (χ, $\dot{\chi}$, η, $\dot{\eta}$) to the so-called van der Pol co-ordinates

(X, Φ, H, Ψ) (see Roberts and Spanos [16]). Then

$$\begin{aligned} \chi(t) &= X(t)\sin\Phi(t), \\ \dot{\chi}(t) &= \Omega X(t)\cos\Phi(t), \\ \eta(t) &= H(t)\sin\Psi(t), \\ \dot{\eta}(t) &= \Omega H(t)\cos\Psi(t), \end{aligned} \tag{11}$$

$$\Phi(t) = \Omega t + \varphi(t), \quad \Psi(t) = \Omega t + \psi(t). \tag{12}$$

Here $X(t)$, $H(t)$, $\varphi(t)$ and $\psi(t)$ are assumed to vary with a time scale that is large compared to the vibration period $T = 2\pi/\Omega$ which is the characteristic time scale for the change of $\Phi(t)$ and $\Psi(t)$. Of course, a harmonic solution represented by equations (11) implies that the amplitude and phase variables are constant with time.

From equations (11) the following so-called consistency conditions are derived:

$$\begin{aligned} \dot{Q}\sin\Phi + Q\cos\Phi\dot{\varphi} &= 0, \\ \dot{H}\sin\Psi + H\cos\Psi\dot{\psi} &= 0. \end{aligned} \tag{13}$$

Consider a linear viscous system driven by the harmonic excitation $F_0\cos(\Omega t + \theta)$ such as system (9) with $\zeta_1 = v = 0$. At resonance where $\Omega = \omega_0$ the velocity is given as $\dot{\chi}(t) = (1/2\zeta_0\omega_0)F_0\cos(\omega_0 t + \theta)$. Hence, the velocity and the excitation are in phase. In the following this is assumed to be the case also for the actual system (9) with the non-linear self-induced damping term and control force included, i.e., $\theta \approx \varphi$. Inserting equations (11) into system (9) then provides

$$\begin{aligned} &\Omega\dot{X}\cos\Phi - \Omega X\sin\Phi(\Omega + \dot{\varphi}) + 2\omega_0\left(\zeta_0 - \zeta_1\left(1 - \varepsilon_D\frac{X^2\sin^2\Phi}{D^2}\right)\right)\Omega X\cos\Phi \\ &\quad + \omega_0^2 X\sin\Phi = v\omega_c H(\omega_c\sin\Psi + 2\zeta_c\Omega\cos\Psi) + F_0\cos\Phi, \end{aligned} \tag{14}$$

$$\begin{aligned} &\Omega\dot{H}\cos\Psi - \Omega H\sin\Psi(\Omega + \dot{\psi}) \\ &\quad + (2\zeta_c\omega_c\Omega\cos\Psi + \omega_c^2\sin\Psi)H = (\omega_c^2\sin\Phi + 2\zeta_c\omega_c\Omega\cos\Phi)X. \end{aligned} \tag{15}$$

Equations (13)–(15) represent four coupled differential equations in X, φ, H, ψ. It is possible to solve these equations for the time derivative of amplitude and phase variables in the following form:

$$\begin{aligned} \dot{X} = {} &\frac{\Omega^2 - \omega_0^2}{\Omega}\cos\Phi\sin\Phi X - 2\omega_0\left(\zeta_0 - \zeta_1\left(1 - \varepsilon_D\frac{X^2\sin^2\Phi}{D^2}\right)\right)X\cos^2\Phi \\ &+ \frac{v\omega_c}{\Omega}\cos\Phi(\omega_c\sin\Psi + 2\zeta_c\Omega\cos\Psi)H + \frac{1}{\Omega}F_0\cos^2\Phi, \end{aligned} \tag{16}$$

$$\begin{aligned} \dot{\varphi} = {} &\frac{\omega_0^2 - \Omega^2}{\Omega}\sin^2\Phi + 2\omega_0\left(\zeta_0 - \zeta_1\left(1 - \varepsilon_D\frac{X^2\sin^2\Phi}{D^2}\right)\right)\cos\Phi\sin\Phi \\ &- \frac{v\omega_c}{\Omega}\sin\Phi(\omega_c\sin\Psi + 2\zeta_c\Omega\cos\Psi)\frac{H}{X} + \frac{1}{\Omega X}F_0\cos\Phi\sin\Phi, \end{aligned} \tag{17}$$

$$\dot{H} = \frac{\Omega^2 - \omega_c^2}{\Omega} \cos \Psi \sin \Psi H - 2\zeta_c \omega_c H \cos^2 \Psi$$

$$+ \frac{\omega_c}{\Omega} \cos \Psi (\omega_c \sin \Phi + 2\zeta_c \Omega \cos \Phi) X, \tag{18}$$

$$\dot{\psi} = \frac{\omega_c^2 - \Omega^2}{\Omega} \sin^2 \Psi + 2\zeta_c \omega_c \cos \Psi \sin \Psi - \frac{\omega_c}{\Omega} \sin \Psi (\omega_c \sin \Phi + 2\zeta_c \Omega \cos \Phi) \frac{X}{H}, \tag{19}$$

where $X(t)$, $H(t)$, $\varphi(t)$ and $\psi(t)$ are functions that vary slowly with time. Hence, the long-term variation of $\dot{X}$, $\dot{\varphi}$, $\dot{H}$, $\dot{\psi}$ is not controlled by the instantaneous value of the right-hand sides in equations (16)–(19), but merely depends on the average value over a vibration period $T = 2\pi/\Omega$.

This observation is used in the so-called averaging method or Kryloff–Bogoliuboff–Mitropolsky first order perturbation method [17], where the right-hand sides in equations (16)–(19) are replaced by their average values over T as the slowly varying parameters X, φ, H, ψ are assumed to be constant over the period. Thus, equations (16)–(19) reduce to

$$\dot{X} = -\omega_0 \left(\zeta_0 - \zeta_1 \left(1 - \frac{\varepsilon_D}{4} \frac{X^2}{D^2} \right) \right) X$$

$$+ \frac{\nu \omega_c}{2\Omega} (-\omega_c \sin \varphi_0 + 2\zeta_c \Omega \cos \varphi_0) H + \frac{1}{2\Omega} F_0, \tag{20}$$

$$\dot{\varphi} = \frac{1}{2} \frac{\omega_0^2 - \Omega^2}{\Omega} - \frac{\nu \omega_c}{2\Omega} (\omega_c \cos \varphi_0 + 2\zeta_c \Omega \sin \varphi_0) \frac{H}{X}, \tag{21}$$

$$\dot{H} = -\zeta_c \omega_c H + \frac{1}{2} \frac{\omega_c}{\Omega} (\omega_c \sin \varphi_0 + 2\zeta_c \Omega \cos \varphi_0) X, \tag{22}$$

$$\dot{\varphi} = \frac{1}{2} \frac{\omega_c^2 - \Omega^2}{\Omega} - \frac{1}{2} \frac{\nu \omega_c}{\Omega} (\omega_c \cos \varphi_0 - 2\zeta_c \Omega \sin \varphi_0) \frac{X}{H}. \tag{23}$$

Here φ_0 denotes the relative phase shift between the motion of the primary and the secondary system, i.e., $\varphi_0 = \varphi - \psi$. φ_0 is expected to approach $\pi/2$ as the frequency tuning ω_c/ω approaches the optimal value. This is true, since optimal damping of the vibration occurs if the force of inertia of the secondary system, $-m_c \ddot{\eta}$, is acting in a direction opposite to the velocity of the primary system, $\dot{\chi}$, in the harmonic motion. Referring to equations (11) this requires

$$\Omega^2 H \sin(\Omega t + \psi) = -a \Omega X \cos(\Omega t + \varphi), \tag{24}$$

where a is a positive constant. By equation (24) it is concluded that the phase shift must be $\varphi_0 = \varphi - \psi \cong \pi/2$ for optimal damping.

Possible harmonic motions are obtained when $\dot{X} = \dot{\varphi} = \dot{H} = \dot{\psi} = 0$ which leads to the non-linear algebraic equations

$$-\omega_0 \left(\zeta_0 - \zeta_1 \left(1 - \frac{\varepsilon_D}{4} \frac{X^2}{D^2} \right) \right) X + \frac{\nu \omega_c}{2\Omega} (-\omega_c \sin \varphi_0 + 2\zeta_c \Omega \cos \varphi_0) H + \frac{1}{2\Omega} F_0 = 0, \tag{25}$$

$$(\omega_0^2 - \Omega^2) X - \nu \omega_c (\omega_c \cos \varphi_0 + 2\zeta_c \Omega \sin \varphi_0) H = 0, \tag{26}$$

$$-\zeta_c H + \frac{1}{2\Omega}(\omega_c \sin\varphi_0 + 2\zeta_c \Omega \cos\varphi_0) X = 0, \tag{27}$$

$$(\omega_c^2 - \Omega^2) H - \omega_c(\omega_c \cos\varphi_0 + 2\zeta_c \Omega \sin\varphi_0) X = 0. \tag{28}$$

Equations (25)–(28) represent four coupled algebraic equations for the determination of the unknown circular vibration frequency, Ω, the amplitudes of the primary and the secondary system, X and H, and the phase shift, φ_0.

In the absence of the F_0 term, equations (25)–(28) are fulfilled for

$$X = H = 0. \tag{29}$$

The solution (29) indicates that the vortex-induced motion is completely damped. This solution, which will be further analysed below, is possible only because the additive, external load has been disregarded. Notice that Ω and φ_0 are not determined in this case. Next, assume that $X \neq 0 \wedge H \neq 0$. Solving equations (27) and (28) with respect to $\sin\varphi_0$ and $\cos\varphi_0$ provides

$$\begin{bmatrix} \sin\varphi_0 \\ \cos\varphi_0 \end{bmatrix} = \frac{H/X}{\omega_c(\omega_c^2 + 4\zeta_c^2\Omega^2)} \begin{bmatrix} 2\zeta_c\Omega^3 \\ 4\zeta_c^2\omega_c\Omega^2 + \omega_c(\omega_c^2 - \Omega^2) \end{bmatrix}. \tag{30}$$

From equation (30) the following solution is obtained for φ_0:

$$\tan\varphi_0 = \frac{2\zeta_c\Omega^3}{4\zeta_c^2\omega_c\Omega^2 + \omega_c^3 - \omega_c\Omega^2}. \tag{31}$$

The ratio H/X follows from equation (27):

$$\frac{H}{X} = \frac{1}{2\zeta_c\Omega}(\omega_c \sin\varphi_0 + 2\zeta_c\Omega\cos\varphi_0). \tag{32}$$

Insertion of equation (32) into equation (26) provides the following relation between Ω and φ_0:

$$\omega_0^2 - \Omega^2 = \frac{v\omega_c}{2\zeta_c\Omega}(\omega_c\cos\varphi_0 + 2\zeta_c\Omega\sin\varphi_0)(\omega_c\sin\varphi_0 + 2\zeta_c\Omega\cos\varphi_0)$$

$$\Rightarrow \omega_0^2 - \Omega^2 = v\omega_c^2 + \left(\frac{v\omega_c^3}{2\zeta_c\Omega} + 2v\zeta_c\omega_c\Omega\right)\sin\varphi_0\cos\varphi_0. \tag{33}$$

Inserting equation (31) into equation (33), a polynomial equation of the fourth degree in Ω^2 is obtained in the form

$$p_4\Omega^8 + p_3\Omega^6 + p_2\Omega^4 + p_1\Omega^2 + p_0 = 0, \tag{34}$$

and

$$\begin{aligned} p_4 &= -4\zeta_c^2, \quad p_3 = 4\zeta_c^2\omega_0^2 - 16\zeta_c^4\omega_c^2 - \omega_c^2 + 8\zeta_c^2\omega_c^2 - 16v\zeta_c^4\omega_c^2, \\ p_2 &= 16\zeta_c^4\omega_0^2\omega_c^2 + \omega_0^2\omega_c^2 - 8\zeta_c^2\omega_0^2\omega_c^2 - 8\zeta_c^2\omega_c^4 + 2\omega_c^4 - 16v\zeta_c^4\omega_c^4, \\ p_1 &= 8\zeta_c^2\omega_0^2\omega_c^4 - 2\omega_0^2\omega_c^4 - \omega_c^6 - 8v\zeta_c^2\omega_c^6 + v\omega_c^6, \quad p_0 = \omega_0^2\omega_c^6 - v\omega_c^8. \end{aligned} \tag{35}$$

Equation (34) has four potential solutions with respect to Ω^2. However, two of the solutions are mutually complex conjugated and one is negatively real. Only one positive, real root exists, which is the root of physical significance. In the following, Ω signifies the positive square root of this solution.

For the amplitude of the primary system a polynomial of the third degree is determined from equation (25),

$$p_3^* X^3 + p_2^* X^2 + p_1^* X + p_0^* = 0, \tag{36}$$

where

$$p_3^* = -\zeta_1 \omega_0 \frac{\varepsilon_D}{4D^2}, \quad p_2^* = 0,$$

$$p_1^* = \frac{v\omega_c}{4\zeta_c \Omega^2}(4\zeta_c^2 \Omega^2 \cos^2 \varphi_0 - \omega_c^2 \sin^2 \varphi_0) + \omega_0(\zeta_1 - \zeta_0), \quad p_0^* = \frac{1}{2\Omega} F_0. \tag{37}$$

Equation (36) predicts up to three real solutions each of which corresponds to a possible harmonic solution with the circular frequency Ω.

For $C_L = 0$, the roots to equation (36) are found to be

$$X = \sqrt{\frac{-p_1^*}{p_3^*}}. \tag{38}$$

With X known, H is determined from

$$H = \frac{1}{2\zeta_c \Omega}(\omega_c \sin \varphi_0 + 2\zeta_c \Omega \cos \varphi_0) X. \tag{39}$$

4. NUMERICAL EXAMPLE

The above method will be applied to the Rio–Niterói Bridge in Rio de Janeiro, Brazil. The greater part of the 14 km long bridge consists of a prestressed concrete structure, whereas the three central spans (700 m) are designed as continuous steel twin-box girders (see Figure 3) with a total weight of 13 100 tonnes [18].

One of the recurring aeroelastic aspects of this flexible and lightly damped long-span steel bridge is its vortex-induced vertical bending motion under relatively low wind velocities. The vortex shedding results in amplitudes about $\pm$ 250 mm (at the centre of the main span) related to the first vertical bending mode. These amplitudes occur when wind velocity approaches 55 km/h. The amplitudes related to the second vertical bending mode are found to be even larger ($\pm$ 300 mm) for wind velocities in the range of 90–120 km/h (see Batista and Pfeil [15]).

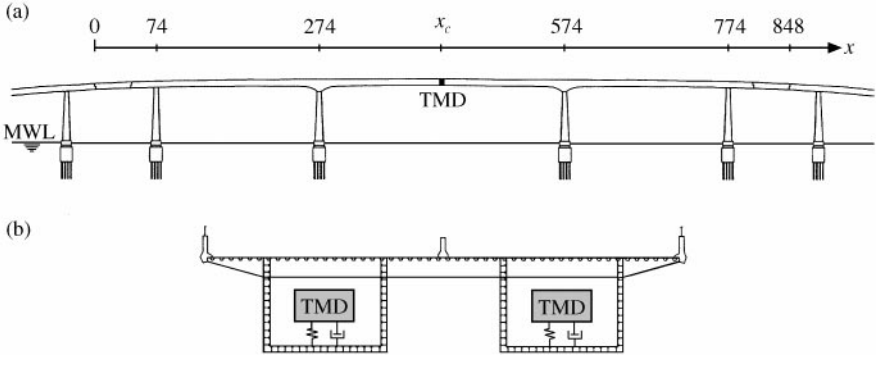

Figure 3. Centre spans of Rio–Niterói bridge. (a) position of tuned mass damper system, (b) tuned mass damper units in the twin steel box girders.

Only the first eigenmode will be considered. The frontal dimension of the bridge, D (i.e. the height of the bridge deck), varies along the longitudinal direction and is estimated for a fixed height of $D = 7{\cdot}5$ m. The natural frequency related to the first eigenmode is 0·32 Hz according to Batista and Pfeil [15]. Furthermore, some modal parameters related to the first eigenmode are determined from a finite element model of the bridge. With reference to the model (9), (10) the following parameters are used:

$$M = 3{\cdot}753 \times 10^3 \text{ kg}, \quad \zeta = 7{\cdot}81 \times 10^{-3}, \quad \alpha_1 = 3{\cdot}288 \times 10^2, \quad \alpha_2 = 2{\cdot}004 \times 10^2,$$
$$\alpha_4 = 1{\cdot}198 \times 10^2, \quad Y_1 = 13, \quad \rho = 1{\cdot}3 \text{ kg/m}^3, \quad U = 18 \text{ m/s}, \; C_L \in [0, 0{\cdot}15]. \tag{40}$$

These parameters correspond to the worst possible combination related to lock-in at the first bending mode. Lift coefficients larger than 0·15 will make the self-induction disappear.

The mode shape is normalized to a maximum value of 1 at the middle of the central span. Hence, the amplitude of the generalized co-ordinate, q, is 250 mm. To fulfil this, ε must be

$$\varepsilon = \frac{\alpha_2}{\alpha_4} \frac{4D^2}{\zeta_1^*} \left(\frac{\zeta_1^* - \zeta}{Q^2} + \frac{F_0^*}{2\omega^2 Q^3} \right), \tag{41}$$

where

$$\zeta_1^* = \frac{\alpha_2 \rho U D Y_1}{4M\omega}, \quad F_0^* = \frac{1}{2M} \alpha_1 \rho U^2 D C_L. \tag{42}$$

The frequency tuning is optimized in the frequency domain using the averaging method. Afterwards, the solution is verified in the time domain (Runge–Kutta integration). In the

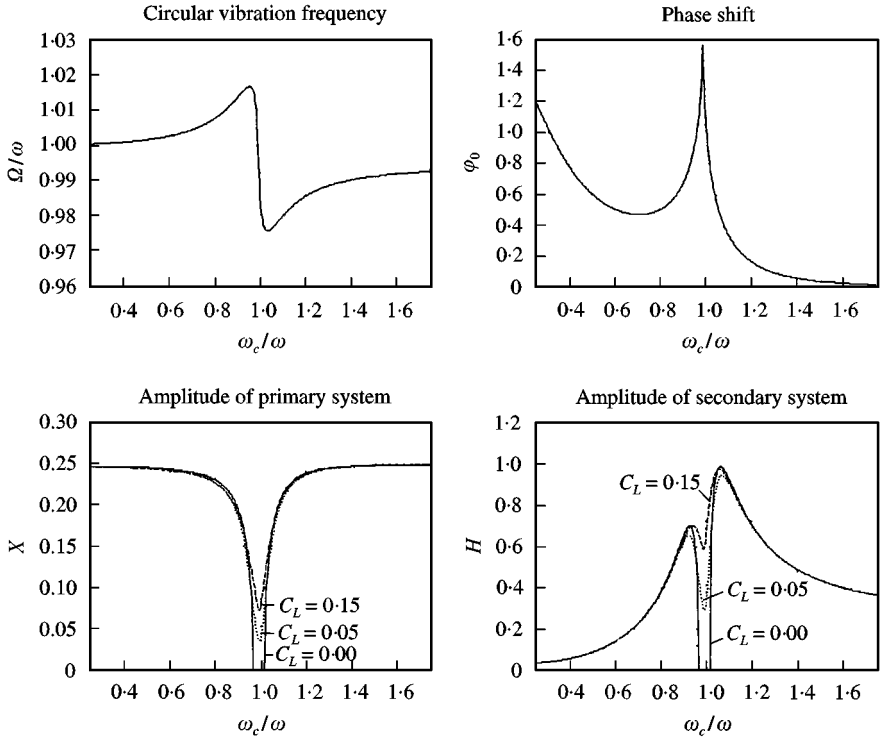

Figure 4. Harmonic response solutions, as a function of the lift coefficient for the first bending eigenmode of Rio–Niterói Bridge with $c_c = c_c^*$ given by equation (43).

example $\nu = 0{\cdot}01$, i.e., $m = 0{\cdot}01M$, and the optimal damping coefficient for a harmonic load will be used, which according to Korenev and Reznikov [14] is given as

$$c_c^* = m_c\omega\sqrt{\frac{3\nu}{2(1+\nu)^3}}. \tag{43}$$

Initially, three solutions with different lift coefficients will be compared, i.e., for $C_L = 0$, 0·05 and 0·15. In Figure 4 the solutions for the circular vibration frequency, the phase shift and the amplitude of both the primary and secondary systems are shown.

For $C_L = 0{\cdot}05$ and 0·15 a single, well-defined solution exists for all values of ω_c/ω, which follows from equations (25)–(28). For $C_L = 0$ a branching to the solution (29) of zero amplitudes for the primary and secondary systems takes place in an interval of ω_c/ω close to 1. The circular frequency and the phase shift are independent of C_L, though it should be noticed that no solutions for these quantities exist when $C_L = 0$. As expected the phase shift φ_0 approaches $\pi/2$ for the optimal frequency tuning. Furthermore, the influence of C_L in the optimal tuning interval is significant. A tripling of C_L results in a doubling of the amplitudes.

The solution $X = H = 0$ in the optimal tuning interval $\omega_c/\omega \in [0{\cdot}9685,\ 1{\cdot}0165]$ is asymptotically orbitally stable. This has been demonstrated by numerical integration of equations (9) as shown in Figure 5 for the left-hand branch of the frequency domain solution. It is seen that a monotonous drift towards the solutions of equations (25)–(28) takes place beyond this interval. It should be noticed that the stability analysis concerns the exact equations of motion and not the averaged differential equations (25)–(28).

It is seen that the zero-amplitude solution is only stable where the other solution does not exist. A similar conclusion can be made for the right-hand branch. Thus, the solution $X = H = 0$ is physically valid only in the interval between the two intersection points.

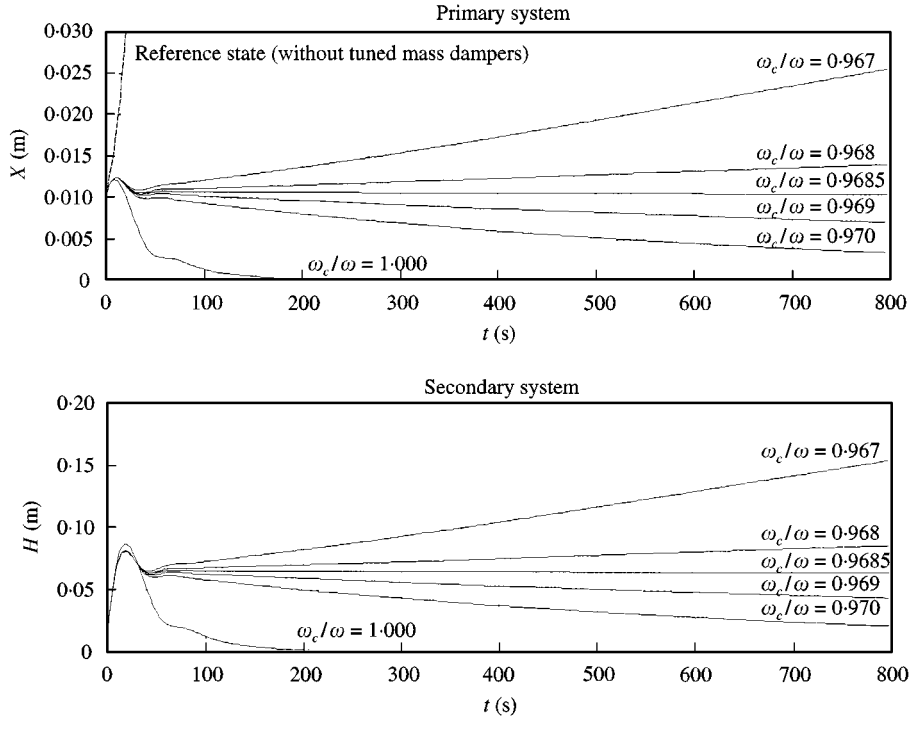

Figure 5. Long-term time development of amplitudes for $C_L = 0$.

Next, the behaviour of the two systems is examined when the damping coefficient is altered from the value given by equation (43). For higher damping coefficients, i.e., $c_c > c_c^*$, there is an unambiguous loss in efficiency. On the other hand, when the damping is lowered three solutions labelled a, b, c may co-exist as illustrated in Figure 6.

As seen in Figure 6, two of the solutions result in higher amplitudes than for the previous solution shown in Figure 4, where the damping coefficient is determined by equation (43), whereas the third solution gives lower amplitudes for frequency tunings around 1. The multiple solutions imply a kind of amplitude hysteresis if the tuning is slowly changed, resulting in jumps from one branch to another. The hysteresis behaviour becomes more noticeable when the damping coefficient is further lowered. In Figure 7 the stability of the indicated solutions has again been studied by numerical integration.

All solutions are stable when the parameters are chosen as stated although the solution corresponding to the lowest amplitudes approaches a steady state motion more slowly than the two other solutions. In contrast, when the damping coefficient is chosen as $c_c = 0{\cdot}14c_c^*$ instead of $c_c = 0{\cdot}16c_c^*$ only the solution predicting the highest amplitude is stable. Comparing Figure 7 and Figure 8 it is observed that the shift between three physically valid solutions and only one physically valid solution depends on the relative position of the solutions for the amplitude response of the secondary system. Thus, the peak of the solution 1 must lie below solution 3 in order to achieve stability for three solutions.

From the above, it might be concluded that the optimal damping coefficient is $c_c = 0{\cdot}16c_c^*$ since this solution gives at best a lower amplitude than the one found using equation (43). However, there is no certainty that the lower of the three amplitude solutions will be obtained in practice. The system might as well oscillate at one of the higher amplitudes.

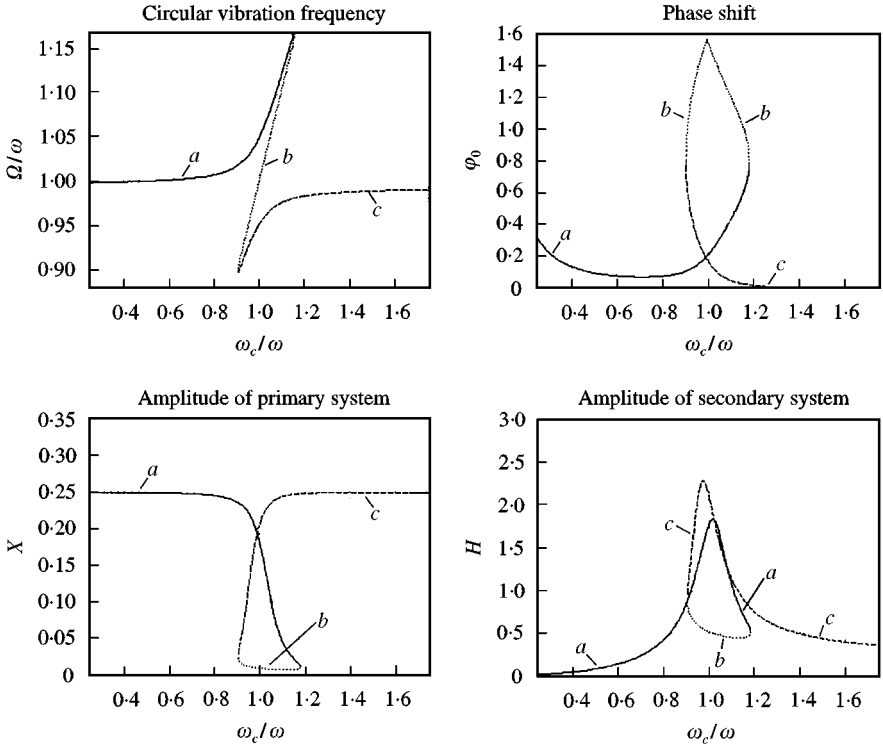

Figure 6. Harmonic response solutions for $C_L = 0{\cdot}15$ and $c_c = 0{\cdot}16c_c^*$.

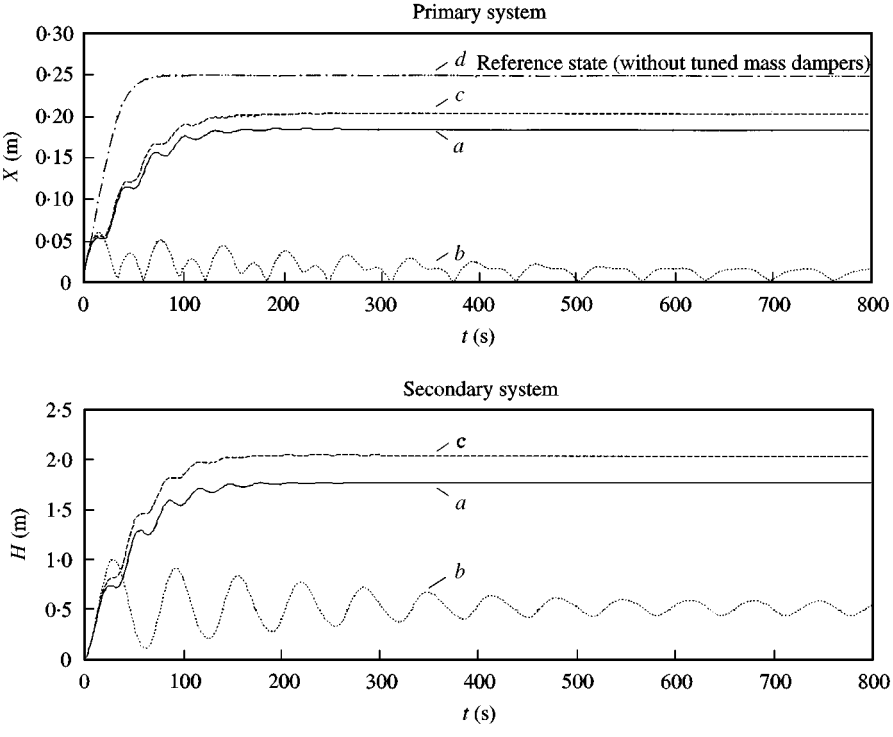

Figure 7. Long-term time development of amplitudes for $\omega_c/\omega = 1$.

Therefore, use of the damping coefficient determined by equation (43) is recommended in order to obtain an unambiguous solution which can be used in the optimization of the mass of the tuned mass dampers.

5. CONCLUSIONS

The present optimization method for tuned mass dampers to one-dimensional slender structures is based on a van der Pol oscillator model for the vortex-induced wind load. When no external additive load is introduced it is possible to reduce the amplitudes of both the primary and secondary system to zero for an interval of the frequency tuning close to 1.

To achieve a more realistic solution it is necessary to include an inhomogeneity in the van der Pol load model. The inhomogeneity is chosen as a harmonic excitation in phase with the velocity of the structure. Then only the amplitudes of the two systems depend on the level of inhomogeneity, whilst the circular vibration frequency and the phase shift are unaffected.

When using the optimal damping coefficient for a strictly harmonic excitation an unambiguous solution is obtained and, thus a single optimal frequency tuning exists for which the reduction in the amplitude of the primary system is greatest. Higher damping coefficients are not beneficial for reducing the amplitude since they result in lower efficiency of the tuned mass damper. The use of low damping coefficients can at best give a lower amplitude than the one tuned mass damper. The use of low damping coefficients can at best give a lower amplitude than the one used for harmonic excitation, but might also result in higher amplitudes. Therefore, it is necessary to use the damping coefficient optimized for harmonic excitation to obtain an unambiguous solution.

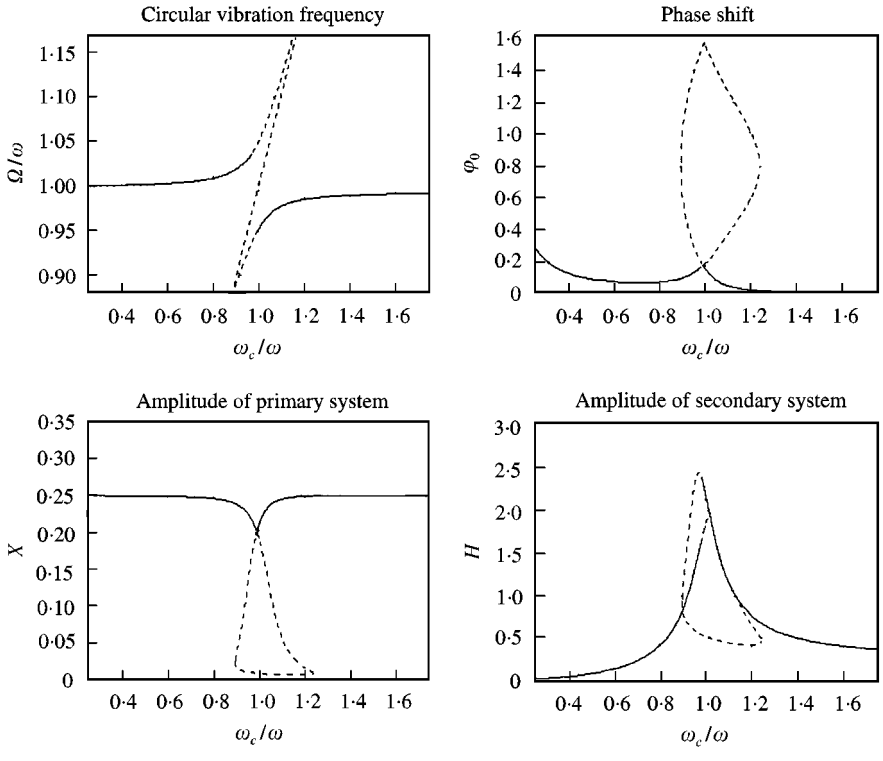

Figure 8. Solutions to the system of equations (25)–(28) for $C_L = 0{\cdot}15$ and $c_c = 0{\cdot}14c_c^*$ in the frequency domain.

In contrast to Batista and Pfeil [15], the total damping of the vibrations of a bridge deck can be achieved merely by using tuned mass dampers when the same Simiu–Scanlan load model is used, that is, a model which does not include any additive load but only a self-induced load from negative aerodynamic damping.

REFERENCES

1. E. SIMIU and R. H. SCANLAN 1996 *Wind Effects on Structures*. New York: John Wiley & Sons Inc.
2. R. D. BLEVINS 1990 *Flow-Induced Vibration*. New York: Van Nostrand Reinhold.
3. R. T. HARTLEN and I. G. CURRIE 1970 *Journal of Engineering Mechanics, ASCE* **96**, 577–591. Lift-oscillator model of vortex induced vibration.
4. R. A. SKOP and O. M. GRIFFIN 1973 *Journal of Sound and Vibration* **27**, 225–233. A model for the vortex-excited resonant response of Bluff cylinders.
5. W. D. IWAN and R. D. BLEVINS 1974 *Journal of Applied Mechanics, ASME* **41**, 581–586. A model for vortex-induced oscillation of structures.
6. T. SARPKAYA 1979 *Journal of Applied Mechanics, AMSE* **46**, 241–258. Vortex-induced oscillations. A selective review.
7. S. KRENK and S. R. K. NIELSEN 1999 *Journal of Engineering Mechanics, ASCE* **125**, 1–9. Energy balanced double oscillator model for vortex-induced vibrations.
8. I. GOSWAMI, R. H. SCANLAN and N. P. JONES 1993 *Journal of Engineering Mechanics, ASCE* **119**, 2270–2287. Vortex-induced vibration of circular cylinders. I: experimental data.
9. I. GOSWAMI, R. H. SCANLAN and N. P. JONES 1993 *Journal of Engineering Mechanics, ASCE* **119**, 2288–2302. Vortex-induced vibration of circular cylinders. II: new model.
10. A. LARSEN 1995 *Journal of Engineering Mechanics, ASCE* **121**, 350–353. Vortex-induced vibration of circular cylinders. II: new model. Discussion by Allan Larsen.

11. C. DYRBYE and S. O. HANSEN 1997 *Wind Loads on Structures*. Chichester: John Wiley & Sons Ltd.
12. J. J. CONNOR and B. S. A. KLINK 1996 *Introduction to Motion Based Design*. Southampton: Computational Mechanics Publications.
13. F. LIVESEY and G. L. LAROSE 1995 *Structural Engineering International, IABSE* **5**, 223–224. Tuned mass dampers for the Great Belt East Bridge.
14. B. G. KORENEV and L. M. REZNIKOV 1993 *Dynamic Vibration Absorbers*. Chichester: John Wiley. & Sons Ltd.
15. R. C. BATISTA and M. S. PFEIL 1996 *Proceedings of the 3rd European Conference on Structural Dynamics EURODYN* '96, Florence, Italy, 5–8 June, 1996, 561–567. Active/passive control of vortex-induced oscillations of Rio-Niterói bridge. A. A. Balkema, Rotterdam, Brookfield.
16. J. B. ROBERTS and P. D. SPANOS 1990 *Random Vibration and Statistical Linearization*. Chichester: John Wiley & Sons Ltd.
17. N. MINORSKY 1962 *Nonlinear Oscillations*. Princeton: Van Nostrand.
18. J. UPSTONE and D. REILY 1979 *Proceedings of the Institution of Civil Engineers* **66**, 227–246. Construction of the navigation spans of the Rio-Niterói Bridge.

APPENDIX A: NOMENCLATURE

Ω_s	circular Strouhal frequency
S	Strouhal number
U	wind velocity
D	across-stream dimension
x	along-span co-ordinate
t	time
z	displacement of structure
ϕ	eigenmode of structure
$q, \dot{q}$	modal displacement and velocity in main system
ζ	modal damping ratio of main system
ω	circular eigenfrequency of main system
M	modal mass of main system
F_c	modal control force on main system
F_a	modal aerodynamic load on main system
$\eta, \dot{\eta}$	displacement and velocity of control system
m_c	control mass
ζ_c	damping ratio of control system
ω_c	circular eigenfrequency of control system
x_c	along-span position of control system
f_a	aerodynamic load
Y_1, Y_2, ε	fitting parameters
K	reduced frequency
C_L	lift coefficient
Ω	circular shedding frequency
θ	phase shift
α_n	mode shape integral parameters ($n = 1, 2, 4$)
$\chi, \dot{\chi}$	displacement and velocity of main system at x_c
$\zeta_0, \zeta_1, \omega_0$	help parameters
v, ε_D, F_0	help parameters
X, Φ	van der Pol co-ordinates for main system
H, Ψ	van der Pol co-ordinates for control system
χ, ψ	time-dependent phase angles
p_n	coefficients in frequency polynomial ($n = 0, 1, 2, 3, 4$)
p_n^*	coefficients in amplitude polynomial ($n = 0, 1, 2, 3$)